Temperature-dependent molecular motions and phase behavior of cholesteryl ester analogues

David H. Croll,[1] Pavanaram K. Sripada, and James A. Hamilton

Biophysics Institute, Housman Medical Research Center, Departments of Medicine and Biochemistry, Boston University School of Medicine, 80 East Concord Street, Boston, MA 02118

Abstract The phase behavior and temperature-dependent molecular motions of three cholesteryl ethers (caproyl, myristyl, oleyl) and a cholesteryl carbonate (oleyl) were characterized. The properties of each ether were qualitatively similar to, but quantitatively different from, those of the corresponding cholesteryl ester. For example, cholesteryl oleyl ether exhibited the same phase transitions as cholesteryl oleate, but at much lower temperatures (e. g., the ether isotropic liquid to cholesteric transition is at 29°C). ^{13}C NMR spectra of ethers in the isotropic liquid and liquid crystalline phases were similar to those of the ester analogue. However, near the liquid to liquid crystalline transition, the steroid ring C3 and C6 linewidths, the C3/C6 linewidth ratio, and the steroid ring rotational correlation times τ_{rx} and τ_{rz} calculated from the linewidths were larger for the ether than the ester analogue. The oleyl carbonate had qualitatively different properties from its analogues (e.g., stable vs. metastable cholesteric and smectic phases). Quantitative results (e.g., relatively long τ_{rx} and τ_{rz} in the isotropic liquid phase) for the carbonate were also distinct from those of both the ester and ether analogues. A comparison of analogues in which the polar linkage is the only structural variable yielded insights into the intermolecular interactions which influence phase behavior.—**Croll, D. H., P. K. Sripada, and J. A. Hamilton.** Temperature-dependent molecular motions and phase behavior of cholesteryl ester analogues. *J. Lipid Res.* 1987. **28:** 1444–1454.

Supplementary key words cholesteryl ether • cholesteryl carbonate • cholesteryl ester • ^{13}C NMR • phase transition • molecular motion

Cholesteryl ethers, cholesteryl carbonates, and cholesteryl esters are structural analogues in which the linkage between the acyl chain and the steroid ring differs **(Fig. 1)**. In neat form, these molecular species exhibit liquid crystalline phases with thermotropic properties that depend both on the acyl chain structure and on the chemical nature of the linkage (1). The ether and carbonate analogues thus can be utilized to further our understanding of the factors that affect the phase behavior and transition temperatures of the biologically important cholesteryl esters.

Cholesteryl esters serve as a transport and storage form of cholesterol in mammals and are also an important component of atherosclerotic lesions (2, 3). In biological systems such as plasma lipoproteins and atherosclerotic plaques, cholesteryl esters may form liquid crystalline phase(s), depending on factors such as the amount of other chemical components dissolved in the cholesteryl ester-rich phase (4, 5). Cholesteryl ethers are not commonly found in mammalian tissues, although the palmityl (16:0) and stearyl (18:0) ethers have been detected in bovine heart (6). Because lipolytic enzymes do not hydrolyze the ether linkage, cholesteryl ethers have been widely used as non-metabolizable cholesteryl ester analogues (7–9). The structural similarities of the cholesteryl ethers and esters make the ethers attractive probes for measuring the uptake and distribution of cholesteryl esters in a variety of biological systems. It is therefore important to compare critically the physical properties of the cholesteryl ether with those of the specific cholesteryl ester for which it is acting as a substitute.

The nature of the acyl chain (the chain length and the position and degree of unsaturation) affects the molecular motions of the cholesteryl ester, particularly in the isotropic liquid near the isotropic to liquid crystalline phase transition (10–13). In this study we have utilized structural analogues to determine the effect of the linkage on the molecular motions. Specifically, we report on ^{13}C NMR studies of liquid and liquid crystalline phases of three cholesteryl ethers [oleyl (18:1), myristyl (14:0) and caproyl (6:0)] and one cholesteryl carbonate [oleyl (18:1)]. Molecular motions in the liquid phase near the liquid→liquid crystalline phase transition are described quantitatively

Abbreviations: $T_{I\rightarrow Ch}$, isotropic liquid to cholesteric liquid crystal phase transition temperature; NOE, nuclear Overhauser enhancement; T_1, spin lattice relaxation time; $\nu_{1/2}$, linewidth; τ_{rz}, rotational correlation time for reorientation of the steroid ring about the long axis of symmetry; τ_{rx}, rotational correlation time for reorientation of the steroid ring about the short non-unique axis; TLC, thin-layer chromatography; HPLC, high performance liquid chromatography; DMF, dimethylformamide.

[1]Current address: Chemistry Department, Regis College, Weston, MA 02193.

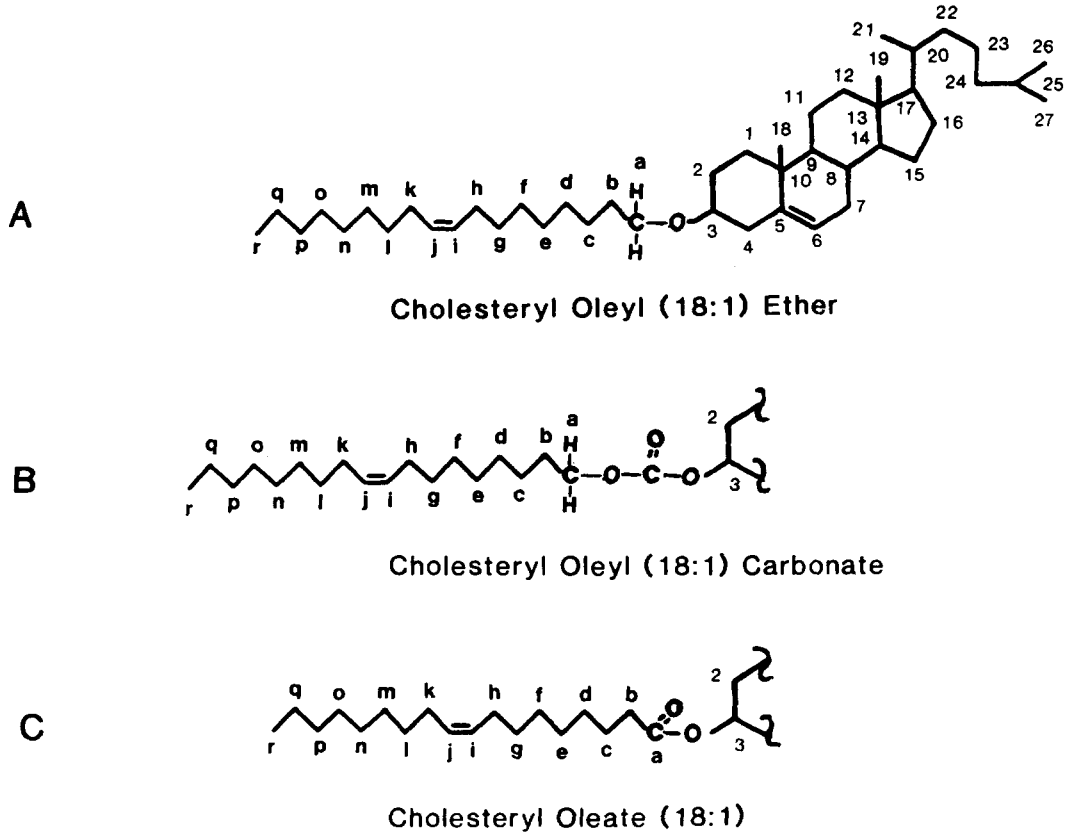

Fig. 1. Structures of A) cholesteryl oleyl (18:1) ether; B) cholesteryl oleyl (18:1) carbonate; C) cholesteryl oleate (18:1) (ester). Steroid ring carbons are numbered according to standard sterol nomenclature; fatty acyl carbons are designated by lower case letters.

and are compared with the analogous cholesteryl ester. In addition, we report the phase behavior of the cholesteryl oleyl ether, based on macroscopic and microscopic observations.

EXPERIMENTAL PROCEDURES

Materials

Cholesteryl *cis*-9,10-octadecenyl carbonate (cholesteryl oleyl carbonate) was purchased from Eastman Kodak Co. (Rochester, NY) and was used without further purification. Mesylates of fatty alcohols and cholesterol were obtained from Nu Chek Prep, Inc. (Elysian, MN). Anhydrous toluene, anhydrous dimethylformamide (DMF), and NaH in 60% oil dispersion were from Aldrich Chemical Co. (Milwaukee, WI). Unisil (activated silicic acid, 100–200 mesh) was from Clarkson Chemical Co., Inc. (Williamsport, PA), and potassium was from Alfa Products (Danvers, MA). TLC plates, silica gel G 5 × 20 cm, 250 microns, were from Analtech (Newark, DE).

Synthesis of cholesteryl ethers

Cholesteryl *cis*-9,10-octadecenyl ether (cholesteryl oleyl ether), cholesteryl tetradecanyl ether (cholesteryl myristyl ether), and cholesteryl hexanyl ether (cholesteryl caproyl ether) were synthesized as follows. The cholesterol anion was generated by heating cholesterol with sodium hydride in mineral oil in anhydrous toluene (14). This reaction mixture was then heated with the mesylate of the desired fatty alcohol in the presence of anhydrous dimethylformamide. This method yielded pure hexyl and oleyl ethers by the criteria of TLC, high performance liquid chromatography, elemental analysis, and ^{13}C NMR spectroscopy (14). However, the tetradecanyl ether contained traces of DMF (detected only by ^{13}C NMR) which were not removed by a single crystallization. Since even trace amounts of impurities affect the phase behavior of thermotropic compounds, the tetradecanyl ether was synthesized by an alternate method in which the cholesterol anion was heated directly with the mesylate of the fatty alcohol, without the use of DMF. This synthesis, as described below in detail, was a slightly modified version of the method previously used to synthesize radiolabeled cholesterol ethers (15, 16).

Cholesterol (270 mg) and potassium were heated in anhydrous toluene for 1 hr under argon. To this was added myristyl mesylate (204 mg) and heating was continued for another 10 hr. The clear supernatant was carefully pipetted off and rotary-evaporated. The residue was taken up in heptane and passed over a column of silicic acid. The

column was eluted with heptane containing increasing amounts of benzene. The cholesteryl tetradecanyl ether was eluted in heptane in fractions containing 15% and 20% benzene. The product was further purified by crystallization from acetone at 0°C. The myristyl ether melted sharply at 50–51°C; the previously reported value was 47–49°C (17). Yields were 55–65%.

Characterization

The purity of the three ethers was checked in two TLC systems, one using hexane–benzene 2:3 and the other hexane–ether 1:1. In both systems the ethers showed a single spot when visualized in an iodine chamber (brown) or when sprayed with sulfuric acid (pink). The purity of the ethers was also verified by elemental analysis, which agreed with the reported values (14).

^{13}C NMR spectra of the compounds in C^2HCl_3 were consistent with their structure (see Results) and revealed no impurities.

The thermotropic phase behavior of the cholesteryl ester analogues **(Table 1)** was determined by inspecting the temperature-dependent macroscopic appearance and texture of the sample (18) as previously described (19). In those cases where previous characterization had not been reported in the literature (cholesteryl oleyl ether and cholesteryl oleyl carbonate), polarizing light microscopy was used to verify phase identification (20).

NMR spectroscopy

Natural abundance proton-decoupled Fourier transform ^{13}C NMR spectra were obtained at 4.7 T (50.3 MHz for ^{13}C) with a Bruker WP-200 spectrometer equipped with an Aspect 2000A data system. Neat samples were contained in a coaxial insert placed in a 10-mm NMR tube containing ^2H_2O as an external lock. Chemical shifts were referenced to the fatty acyl CH_3 (14.10 ppm) of each analogue and are accurate to ±0.05–0.1 ppm.

For spectra of compounds in organic solvent, C^2HCl_3 was used as both solvent and lock substance; $(CH_3)_4Si$ was used as an internal reference. Typically, broadband decoupling (1.0 watt) was centered ~3.4 ppm downfield from the ^1H resonance of $(CH_3)_4Si$. Spectra of the neat lipids were acquired with a 90° pulse (~15.0 μ sec) and a spectral width of 10,000 Hz using 16,384 or 32,768 time domain points, a recycle time of 0.82 sec or 1.64 sec, and 2,000–15,000 accumulations. Spectra of the compounds in C^2HCl_3 were obtained as above, except with 32,768 time domain points and a recycle time of 3.0 sec.

The sample temperatures were controlled to within 1°C with the Bruker B-VT-1000 variable temperature unit. Probe temperature was determined in a sample of ethylene glycol after removal from the probe as described (12). The accuracy of temperature measurement was ±1°C for 25–60°C and ±2°C for higher temperatures. The isotropic liquid to cholesteric liquid crystal phase transition temperature ($T_{I\rightarrow Ch}$) was also accurately determined by visual inspection as previously described (19). Prior to the NMR analysis, samples were melted to the liquid state and kept at 15–20°C above $T_{I\rightarrow Ch}$ for 20–30 min. Spectra were obtained as a function of decreasing temperature after a 20-min thermal equilibration in the NMR probe at each temperature. After NMR experiments conducted at temperatures near (within 3°C) $T_{I\rightarrow Ch}$, the sample was ejected from the probe for visual inspection.

Spin-lattice relaxation time (T_1) values were measured by the fast inversion recovery method (21) and calculated using a program supplied by Bruker Co. which utilized a nonlinear three-parameter fit (22). Nuclear Overhauser enhancement (NOE) was measured as the ratio of peak height in the spectrum obtained with continuous broadband decoupling to that obtained with gated decoupling. To assure that both spectra were obtained at the same temperature, free induction decays under both decoupling conditions were alternately summed at separate computer addresses (12). In all cases, peaks in both spectra had similar lineshapes and linewidths ($\nu_{1/2}$). Calculations of theoretical $\nu_{1/2}$, T_1, and NOE values were performed on a Digital Equipment Corporation LSI-11/2 computer using a modeling program by Quinn (11).

TABLE 1. Thermal transitions of cholesteryl esters and their analogues

Compound	Crystal mp (°C)[a]	Liquid Crystal Transitions (°C)[a,b]
Cholesteryl myristate (14:0)	72	85 I→Ch 80 Ch→Sm
Cholesteryl myristyl (14:0) ether	50	65 I→Ch 58 Ch→Sm
Cholesteryl oleate (18:1)	51	46 I→Ch 42 Ch→Sm
Cholesteryl elaidyl (18:1) ether[c]	48	36.5 I→Ch 26.5 Ch→Sm
Cholesteryl oleyl (18:1) ether	36	29 I→Ch 23 Ch→Sm
Cholesteryl oleyl (18:1) carbonate	~0[d]	31 I→Ch 24 Ch→Sm
Cholesteryl caproate (6:0)	100	102 I→Ch
Cholesteryl caproyl ether (6:0)	68	81 I→Ch

[a] Temperatures ± 1°C. Liquid crystalline phase transition temperatures obtained by visual inspection on cooling. Crystal melting point obtained by visual inspection, except as noted.
[b] I, isotropic liquid; Ch, cholesteric phase; Sm, smectic phase.
[c] Data from Ref. 1.
[d] Measured by differential scanning calorimetry on a sample which was heated from −25°C.

RESULTS

Chemical shift assignments

Fig. 2 shows the natural abundance ^{13}C NMR spectrum of cholesteryl oleyl ether in C^2HCl_3. The expanded aliphatic region demonstrates the high resolution obtained. The ether spectrum was assigned by comparison of chemical shifts with those of the corresponding (oleyl) ester. Compared with the ester, the most notable features of the cholesteryl oleyl ether spectrum were the absence of a carbonyl carbon peak at ~173.6 ppm and the presence of a new peak at 68.2 ppm (from the fatty acyl carbon adjacent to the ether oxygen). Other carbons whose resonances were shifted by proximity to the altered linkage were those of the steroid ring carbons C1 (37.4 ppm), C2 (28.7 ppm), C3 (79.0 ppm), C4 (39.3 ppm), C5 (141.3 ppm), and C6 (121.4 ppm) as well as fatty acyl carbons b (30.2 ppm) and c (26.3 ppm). **Table 2** gives assignments and chemical shifts for all carbons affected by linkage alteration. The chemical shifts for the remaining carbons were unaffected (±0.1 ppm) by the alteration of the linkage.

The ^{13}C spectrum of cholesteryl oleyl carbonate in C^2HCl_3 (not shown) was nearly identical to that of cholesteryl oleate except for resonances from carbons near the steroid ring–acyl chain linkage. The most notable changes (Table 2) were the carbonate carbonyl resonance (154.7 ppm), which was shifted ~20 ppm upfield from the ester carbonyl, and the acyl carbon linked to oxygen, which appeared at 67.9 ppm (~0.3 ppm from the analogous carbon in the ether analogue). In addition, the chemical shift of the C3 steroid ring carbon of the carbonate was unique (Table 2). Note that the steroid ring C5 and C6 chemical shifts of the carbonate were similar to those of the ester and different from those of the ether.

Similarly, the spectra of the acyl saturated (myristyl and caproyl) ethers in C^2HCl_3 were nearly identical to those saturated acyl cholesteryl esters (13) except for the chemical shifts of carbons in the region of the steroid acyl chain linkage. In particular, the steroid ring C3 (79.0 ppm), C4 (39.3 ppm), C5 (141.3 ppm), C6 (121.4 ppm), and C2 [28.6 ppm (14:0); 28.7 ppm (6:0)] carbons were shifted from their positions in the analogous ester. As expected, the carbonyl resonance observed for the ester

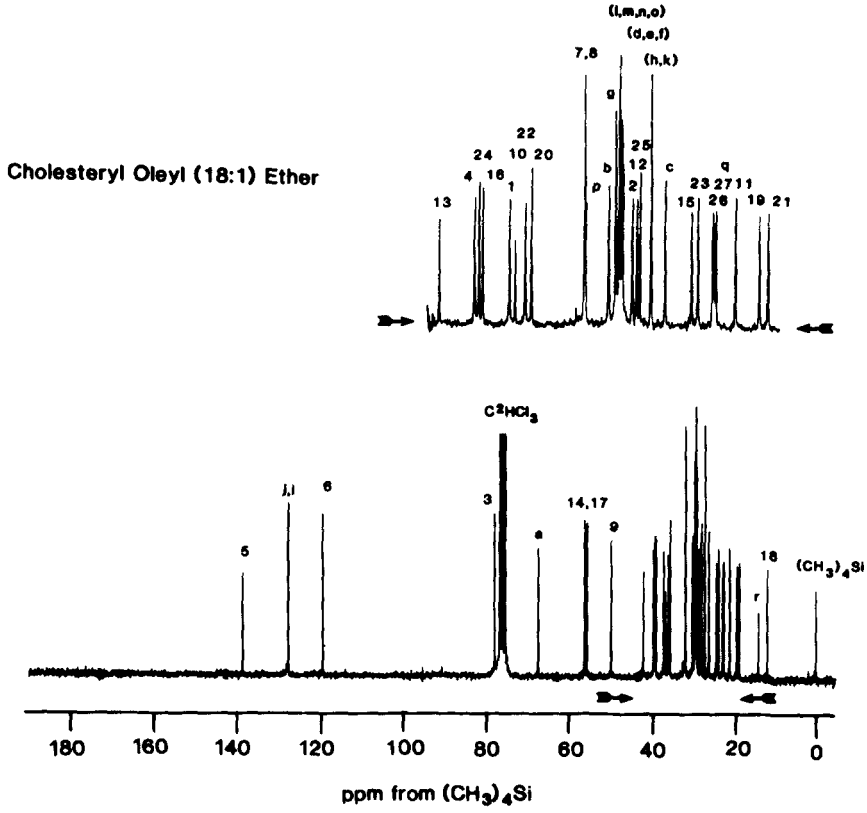

Fig. 2. Proton-decoupled natural abundance ^{13}C Fourier transform NMR spectrum at 50.3 MHz of cholesteryl oleyl ether in C^2HCl_3. Spectrum was recorded after 12,000 (3.0 sec recycle time) accumulations using a 90° (~15 μ sec) pulse with a 10,000 Hz spectral width. The free induction decay (32,768 time domain points) was processed using 0.5 Hz linebroadening. Assignments are shown for steroid ring carbons (numbered by standard sterol nomenclature) and for fatty acyl carbons (lower case letters).

TABLE 2. Selected[a] assignments and chemical shifts in ppm from $(CH_3)_4Si$ for cholesteryl ester analogues in C^2HCl_3

Atom	Cholesteryl Oleate	Cholesteryl Oleyl Ether	Cholesteryl Oleyl Carbonate
C1	37.1	37.4	38.1
C2	27.9	28.7	27.8
C3	73.3	79.0	77.7
C4	38.2	39.3	39.6
C5	139.8	141.3	139.5
C6	122.7	121.4	122.9
C9	50.1	50.4	50.1
C10	36.6	37.0	36.6
a	173.2	68.2	67.7
b	34.7	30.2	36.9
c	25.1	26.3	25.8
Carbonate			154.7

[a]Assignments and chemical shifts listed are carbons for which the chemical shift differed by >0.2 ppm in the three analogues.

(173.3 ppm) was absent, and a resonance from the acyl methylene proximal to the ether oxygen was present (68.3 ppm). Also, fatty acyl carbon resonances b [30.2 ppm (6.0); 30.3 ppm (14.0)] and c [25.9 ppm (6:0), 26.2 ppm (14:0)] were shifted compared to the analogous esters (13). The chemical shifts of all other carbon resonances were unchanged (± 0.1 ppm) from those of the analogous ester compounds (13).

Thermal characterization

The phase behavior of the cholesteryl ethers and carbonate are summarized and compared with those of the analogous cholesteryl esters in Table 1. The phase transition temperatures of the saturated (6:0 and 14:0) cholesteryl ethers were in good agreement with previous results (1). Compared with the corresponding ester, the same liquid crystalline mesophases were observed but the transition temperatures of the two ethers were much lower (~20°C) than the corresponding esters. Note that the 18:1 ether previously studied (1) was the *trans* compound, cholesteryl elaidyl ether. The *cis* 18:1 ether, cholesteryl oleyl ether, melted at a much lower temperature (~12°C) than the *trans* (18:1) ether. The isotropic to cholesteric transition temperature was ~7°C lower and the cholesteric to smectic transition temperature ~4°C lower for the *cis* (18:1) oleyl ether.

Cholesteryl oleyl ether exhibited the same phases observed for cholesteryl oleate but at lower (15–20°C) temperatures (Table 1). In both cases the liquid crystalline phases are metastable, i.e., they form at temperatures below the crystal melting temperature from the undercooled liquid (23). In contrast, cholesteryl oleyl carbonate exhibited stable smectic and cholesteric liquid crystalline phases. The cholesteric-smectic and isotropic-cholesteric transition temperatures of the carbonate were similar to those of the ether.

Temperature-dependent molecular motions

Fig. 3 shows natural abundance ^{13}C NMR spectra of neat cholesteryl myristyl ether in liquid and liquid crystalline phases. Spectra of the isotropic liquid (Fig. 3A) contained many well-resolved resonances from both steroid ring carbons and the fatty acyl chain, although the resolution was diminished compared to that for the cholesteryl ethers in organic solvent, as expected. On decreasing the temperature from 10°C above $T_{I\rightarrow Ch}$ to 1°C above $T_{I\rightarrow Ch}$ (Fig. 3B), many steroid ring carbon resonances, such as the C6, C3, C14, 17, and C9, broadened significantly. Other resonances such as those from the fatty acyl carbons (including the carbon next to the ether oxygen) and the steroid ring methyl carbons C18, C19, and C21 broadened to a lesser extent.

Upon lowering the sample temperature below $T_{I\rightarrow Ch}$ (Fig. 3C) the spectrum changed abruptly. All steroid ring resonances, as well as the fatty acyl chain resonances proximal to the steroid ring (e.g., the fatty acyl ether-linked carbon) broadened beyond detection. The envelope of resonances from the fatty acyl carbons in the middle of the chain broadened substantially. Only resonances from the distal portion of the fatty acyl chain (and possibly the C26 and C27 of the steroid isooctyl side chain) remained narrow enough to be reasonably well resolved. Concomitant with the cholesteric to smectic phase transition (Fig. 3D) these acyl peaks underwent further broadening and only the resonances from the penultimate methylene and terminal methyl carbons of the acyl chain remained detectable as resolved resonances.

Cholesteryl caproyl ether exhibited temperature-dependent spectra (not shown) similar to those shown for the myristyl ether. The spectra of both compounds exhibited temperature-dependent broadening in the isotropic and liquid crystalline phases which was qualitatively similar to that previously reported for the corresponding cholesteryl esters (13). The oleyl analogues also had temperature-dependent spectra (not shown) which qualitatively paralleled that of cholesteryl oleate[2] (10–12).

Fig. 4 shows plots of the C3 and C6 $\nu_{1/2}$ value and their ratios as a function of temperature relative to $T_{I\rightarrow Ch}$ for the saturated acyl cholesteryl ethers. As $T_{I\rightarrow Ch}$ was approached, the C3 linewidth increased to a greater extent than the C6 linewidth, giving an approximately twofold increase (from 1.2–2.2 over a range of 7–10°C) in the C3/C6 $\nu_{1/2}$ ratio. The C3 and C6 $\nu_{1/2}$ of the unsaturated analogues **(Fig. 5)** (cholesteryl oleyl ether, cholesteryl oleyl carbonate) exhibited much larger values in the isotropic liquid than the saturated ethers. Further, the

[2]Cholesteryl oleyl ether and cholesteryl oleyl carbonate both have a smectic phase which exists in a temperature range well below ambient probe temperature for the NMR spectrometer, and smectic phase spectra of these compounds were not obtained.

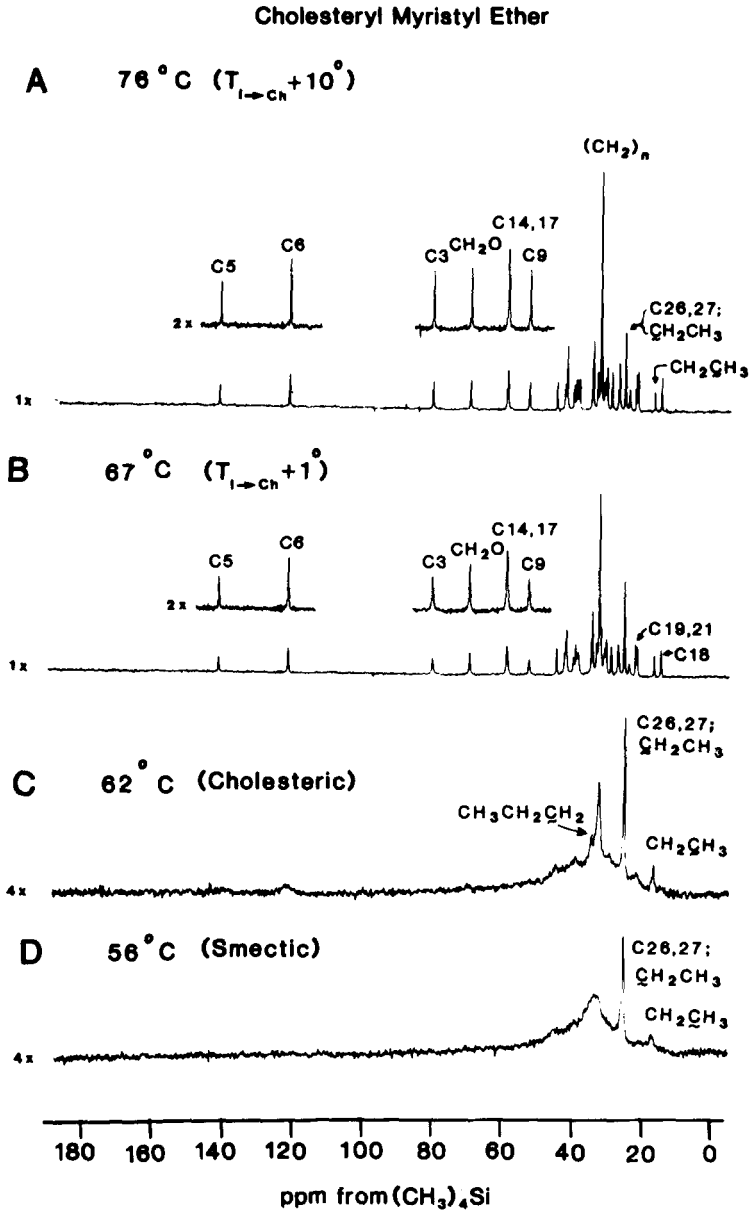

Fig. 3. Proton-decoupled natural abundance ^{13}C Fourier transform NMR spectra at 50.3 MHz of neat cholesteryl myristyl ether. All spectra were recorded after 2,000 accumulations with a 10,000 Hz spectral width and were processed with 1.0 Hz linebroadening (isotropic liquid) or 3.0 Hz linebroadening (liquid crystalline phases). Assignments are shown for selected steroid ring carbons by number (standard sterol nomenclature) and for selected prominent fatty acyl chain carbons as indicated. A) isotropic liquid at $T_{I\rightarrow Ch}$ + 10°C; B) isotropic liquid at $T_{I\rightarrow Ch}$ + 1°C; C) cholesteric phase; D) smectic phase.

C3/C6 linewidth ratios of both analogues (Fig. 5) exhibited a larger increase as $T_{I\rightarrow Ch}$ was approached (e.g., cholesteryl oleyl ether, C3 ν½/C6 ν½ from 2.6 to 4.0 over a range of 10°C), indicating a marked increase in the motional anisotropy of steroid ring reorientation.

The C3 and C6 ν½ values were used to obtain correlation times (τ_{rx}/τ_{rz}) for the rotational reorientation of the steroid ring about the short non-unique axis (τ_{rx}) and the long molecular axis (τ_{rz}) of symmetry for cholesteryl esters, as defined by Quinn (11), using the spectral density functions for a prolate ellipsoid undergoing anisotropic reorientation (24). Since the C3 and C6 are part of a rigid ring system and the C3-H and C6-H angles and bond distances should be the same in cholesteryl esters and their ether and carbonate analogues, the semiquantitative and quantitative treatments applied previously to cholesteryl esters will be applicable to the ether and carbonate molecules. **Table 3** presents experimental T_1 and ν½ values,

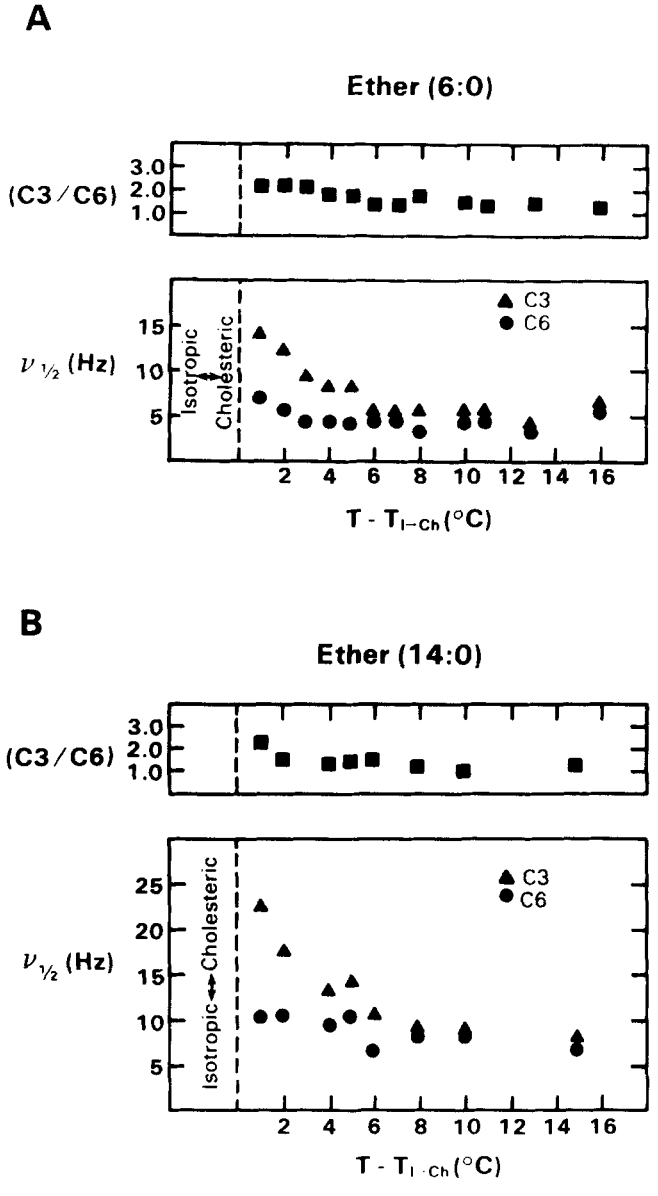

Fig. 4. Plots of the linewidth (ν½) of the C3 (▲) and C6 (●) steroid ring resonances of A) cholesteryl caproyl (6:0) ether versus T-$T_{I\rightarrow Ch}$, the temperature relative to the isotropic liquid to cholesteric liquid crystal phase transition temperature ($T_{I\rightarrow Ch}$) and B) cholesteryl myristyl (14:0) ether. The phase transition is represented by the dashed vertical line. Plots of the linewidth ratio C3 ν½/C6 ν½ versus T-$T_{I\rightarrow Ch}$, the temperature relative to the liquid to liquid crystalline phase transition are shown above the respective linewidth plots.

calculated correlation times, and the motional anisotropy (τ_{rx}/τ_{rz}) for the three cholesteryl ethers and cholesteryl oleyl carbonate. Values for cholesteryl esters (12, 13) are also presented. The measured T_1 values (Table 3) were essentially identical to T_1 values calculated from the correlation times in Table 3. Note also that the C3 and C6 T_1 values are nearly insensitive to both temperature and structural variations.

DISCUSSION

This study contrasts the phase behavior of cholesteryl esters, ethers, and carbonates, with special emphasis on the oleate (18:1 *cis*) derivatives. In a comparison of the oleate derivatives (Table 1) using cholesteryl oleate as a reference point, the change to an ether linkage decreases the transition temperature of each phase transition.

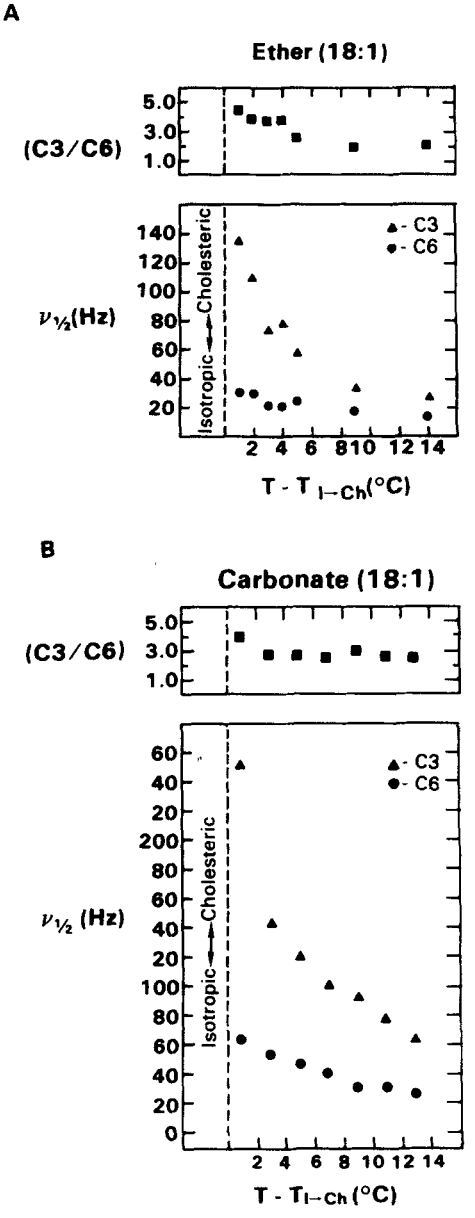

Fig. 5. Plots of the linewidth (ν½) of the C3 (▲) and C6 (●) steroid ring carbons versus T-$T_{I\rightarrow Ch}$, the temperature relative to the isotropic liquid to liquid crystal phase transition temperature for A) cholesteryl oleyl (18:1) ether; B) cholesteryl oleyl (18:1) carbonate. The phase transition is represented by the dashed vertical line. Plots of the linewidth ratio (C3 ν½/C6 ν½) vs. (T-$T_{I\rightarrow Ch}$) are shown above the respective linewidth plots.

TABLE 3. Steroid ring dynamics of cholesteryl ester analogues: experimental C3 and C6 linewidths ($\nu_{1/2}$), linewidth ratios, T_1 and calculated rotational correlation times (τ_{rx}, τ_{rz})

Analogue	Temp. (°C)	C3$\nu_{1/2}$ (Hz)[a]	T1 (s)	C6$\nu_{1/2}$ (Hz)[a]	T1 (s)	C3$\nu_{1/2}$[b] C6$\nu_{1/2}$	τ_{rx} (s)	τ_{rz} (s)	Motional Anisotropy (τ_{rx}/τ_{rz})
Ester (18:1)[c]	$T_{I\to Ch}$ + 1°	60.0	0.12	17.5	0.15	3.4	2.9×10^{-7}	2.8×10^{-9}	103
Cholesteryl oleate	$T_{I\to Ch}$ + 10°	15.8	0.16	7.8	0.12	2.0	6.0×10^{-8}	1.3×10^{-9}	46
Ether (18:1)	$T_{I\to Ch}$ + 1°	136		30.4		4.5	7.0×10^{-7}	4.5×10^{-9}	155
Cholesteryl oleyl ether	$T_{I\to Ch}$ + 9°	33.4		17.5		1.8	1.5×10^{-7}	3.0×10^{-9}	50
Carbonate (18:1)	$T_{I\to Ch}$ + 1°	250	0.20[d]	63	0.15	4.0	1.5×10^{-6}	9.0×10^{-9}	166
Cholesteryl oleyl carbonate	$T_{I\to Ch}$ + 11°	78		30		2.6	4.0×10^{-7}	5.0×10^{-9}	80
Ester (14:0)[e]	$T_{I\to Ch}$ + 1°	14.1	0.21	5.5	0.15	2.6	6.0×10^{-8}	8.5×10^{-10}	71
Cholesteryl myristate	$T_{I\to Ch}$ + 10°	4.3		3.1		1.4	1.5×10^{-8}	3.0×10^{-10}	50
Ether (14:0)	$T_{I\to Ch}$ + 1°	22.4		10.2		2.2	1.0×10^{-7}	1.7×10^{-9}	59
Cholesteryl myristyl ether	$T_{I\to Ch}$ + 10°	8.0		8.0		1.0	2.5×10^{-8}	1.0×10^{-9}	25
Ester (6:0)	$T_{I\to Ch}$ + 1°	6.2		5.5		1.1	1.0×10^{-8}	8.5×10^{-10}	12
Cholesteryl caproate	$T_{I\to Ch}$ + 7°	5.5		4.3		1.3	1.0×10^{-8}	6.0×10^{-10}	17
Ether (6:0)	$T_{I\to Ch}$ + 1°	14.1	0.19	6.8	0.13	2.1	6.0×10^{-8}	8.5×10^{-10}	71
Cholesteryl caproyl ether	$T_{I\to Ch}$ + 10°	5.5	0.18	4.3	0.14	1.3	1.0×10^{-8}	6.0×10^{-10}	17

[a] Linewidths ($\nu_{1/2}$) reported to nearest 1 Hz for $\nu_{1/2} \geq 25$ Hz with error $\leq 10\%$; for $\nu_{1/2} \leq 25$ Hz error ~ 1.2 Hz.
[b] Estimated error $\sim 20\%$ arising from uncertainties in $\nu_{1/2}$.
[c] Data from ref. 12.
[d] T1 estimated from null time in inversion recovery.
[e] Data from ref. 13.

Changing the linkage to a carbonate alters the phase behavior from a metastable to stable system: the crystal melting point decreases greatly, and a crystal to smectic transition occurs at ~ 0°C. The cholesteric→smectic and isotropic→cholesteric transitions for cholesteryl oleyl carbonate occur at temperatures quite similar to those for the corresponding ether. It is significant that all the phase transitions of the *cis* 18:1 ether occur below body temperature, in contrast to those of the *cis* 18:1 ester and the elaidyl (18:1 *trans*) ether (Table 1, ref. 1). Note also that the *trans* 18:1 ether has large temperature ranges for the cholesteric and smectic phases, and that the *cis* 18:1 ether is more analogous to *cis* 18:1 ester in this respect.

Another comparison that merits mention is that of cholesteryl stearate (18:0) with the 18:1 ester and ether. Because of the saturated fatty acyl chain, all the phase transitions of cholesteryl stearate occur well above body temperature (crystal→isotropic, 83°C; isotropic→cholesteric, 79°C; cholesteric→smectic, 72°C; refs. 13, 23). Changing the linkage from ester to ether for the 18:1 analogues results in smaller temperature differences for the corresponding phase transitions (Table 1) than changing the chain unsaturation from zero to one *(cis)* while maintaning the ester linkage. Thus, in terms of phase transition temperatures, cholesteryl oleyl ether is more analogous than cholesterol stearate to cholesteryl oleate.

Changing from the ester linkage to the ether linkage for the myristyl (14:0) and caproyl (6:0) derivatives decreases the temperature of each phase transition but preserves the nature of the phases and phase transitions in both cases (1) (Table 1).

The NMR spectra in C^2HCl_3 show significant linkage-dependent chemical shifts for resonances from steroid ring carbons close to the polar linkage (Table 2). Most of the chemical shifts for corresponding steroid carbons are not altered. Thus, Table 2 shows which carbons are suitable for identifying and/or monitoring a specific molecular type in a mixture of analogues. For example, following introduction of cholesteryl oleyl ether into biological systems, the ether will likely be associated with cholesteryl esters. The carbon resonances listed in Table 2 will allow the ether to be distinguished from the ester. To enhance the detectability of the relatively small amounts of ether in such systems, specific ^{13}C enrichment of an ether carbon such as the steroid ring C4 could be used.

The temperature-dependent ^{13}C NMR spectra of the neat cholesteryl ethers and carbonate were qualitatively similar to those previously recorded for cholesteryl esters (12, 13). For example, spectra of cholesteryl myristyl ether in the isotropic, cholesteric, and smectic phase (Fig. 3) showed the same features as spectra of cholesteryl myristate in the corresponding phases (13). These results imply that molecular motions are relatively unrestricted (though anisotropic; see below) in the liquid phase and highly restricted in the liquid crystalline phases. The qualitative similarity of NMR results for the ethers and esters is consistent with findings by low-angle X-ray scattering, which shows similar structures of the smectic

phases of ethers and corresponding esters (1). However, neither high resolution ^{13}C NMR nor low-angle X-ray scattering provides detailed structural information about the liquid crystalline phases (13).

Although the phase-dependent NMR spectra were qualitatively similar for the different analogues, steroid ring molecular motions (and the relevant NMR quantities, the steroid ring C3 and C6 linewidths) of liquid ethers, esters, and the carbonate were significantly different. The plot of the C3 and C6 linewidth versus reduced temperature for cholesteryl oleyl ether (Fig. 5A) generally resembles that for cholesteryl oleate (12). However, the C3 and C6 linewidths and the correlation times τ_{rx} and τ_{rz} (Table 3) are ~2 times larger for the ether than the ester; the motional anisotropy (τ_{rx}/τ_{rz}) is the same at $T_{I\rightarrow Ch} + 10°$ but is 1.5 times greater at $T_{I\rightarrow Ch} + 1°C$ for the ether.

The most direct consequence of substituting an ether linkage for the ester linkage in cholesteryl oleate is a sizeable reduction in phase transition temperatures (Table 2). The somewhat slower and more anisotropic motions near $T_{I\rightarrow Ch}$ for the ether may be partly a consequence of the lower phase transition temperature (13). Previous NMR results for cholesteryl esters with different chain lengths (and consequently different isotropic liquid→liquid crystalline phase transition temperatures) have shown a general correlation between decreasing temperature and increasing linewidths and correlation times (12, 13). Also, when the isotropic to cholesteric phase transition temperature of cholesteryl oleate is decreased by the addition of small amounts of triglyceride, increased correlation times are observed at $T_{I\rightarrow Ch} + 1°C$ (19). Mixtures of cholesteryl oleate with 2-3% triolein exhibit liquid→cholesteric liquid crystalline phase transitions at temperatures intermediate between the transition temperature for pure cholesteryl oleate and cholesteryl oleyl ether; the C3 and C6 linewidths and the rotational correlation times τ_{rx} and τ_{rz} at $T_{I\rightarrow Ch} + 1°C$ are intermediate between those of the ether and ester.

In contrast to the 18:1 ester/ether pair, the 18:1 carbonate/ether pair has a similar liquid→liquid crystalline transition temperature, permitting a comparison of molecular motions at the same absolute temperature. At a given temperature, the C3 and C6 linewidth and the C3/C6 linewidth ratio are much larger for the carbonate than the ether (Fig. 5; Table 3).[3] These larger linewidths are a reflection of increased correlation times: at 1° and ~10° above the liquid→liquid crystalline transition temperature, τ_{rx} and τ_{rz} are ~twofold larger than τ_{rx} and τ_{rz} of the ether. A quantitative comparison with previous NMR results (at the same magnetic field) for cholesteryl esters (12, 13, 19) reveals that the results for the carbonate are anomalous in several respects. The carbonate has *i*) the largest C3 and C6 linewidth at any reduced temperature, *ii*) the largest C3/C6 linewidth ratio (>2.5) at temperatures well above $T_{I\rightarrow Ch}$, and *iii*) the longest correlation times and the largest anisotropy ratio (τ_{rx}/τ_{rz}) at 1° and ~10° above $T_{I\rightarrow Ch}$. Thus, the steroid ring motions are relatively restricted and anisotropic as a result of the carbonate linkage, suggesting different intermolecular interactions in the liquid state (see below). Pretransitional changes in physical properties of liquid cholesteryl oleyl carbonate have also been observed by other physical methods (25).

The saturated ethers yielded spectra with much narrower C3 and C6 linewidths and a lower C3/C6 linewidth ratio at any given reduced temperature than the 18:1 ether and carbonate. In these respects, the saturated ethers were similar to the saturated esters (13). The steroid ring motions of the liquid saturated-chain ethers are more rapid and less anisotropic than the motions of the 18:1 ether and carbonate (Table 3).

The present NMR results for the carbonate and ethers can be interpreted with reference to previous NMR studies of cholesteryl esters. Saturated cholesteryl esters, because of stronger intermolecular interactions, readily preorder into a cholesteric phase over a very narrow temperature range just above $T_{I\rightarrow Ch}$, so that preordering is not detected by ^{13}C linebroadening (13). A single *cis* double bond in the acyl chain will distort the linearity of the chain,[4] reducing the chain-chain cooperative interactions in the liquid phase and decreasing the temperature at which the liquid crystalline phase forms; much larger anisotropies and slower motions are seen in the liquid phase (12). Generally similar effects are seen when triolein is added (in small quantities) to cholesteryl esters. We suggested, in this case, that highly anisotropic domains form in the liquid but are inhibited from reaching a critical size and/or concentration by increasing amounts of triglyceride (19). On changing from the ester to the ether analogue, the transition temperatures decrease and the motional anisotropy increases, even though reduction of the polarity of bond should favor stronger hydrophobic intermolecular interactions.[5] It is possible that because of the somewhat smaller bond angle of the ether linkage (~110°

[3]The NMR differences are not attributable to the difference in thermal stability of the mesophases, as previous results for different cholesteryl esters showed that the NMR results for the liquid phase are not dependent on the stability of the cholesteric phase (13).

[4]The least disruptive distortion would be a chain "dislocation" as found in the X-ray crystallographic structures of ω-9 *cis* acyl cholesteryl esters (26).

[5]Ring-ring and chain-chain interactions are thought to be the driving forces for cholesteryl ester liquid crystal formation (12, 23). Of the three 18:1 analogues, the ester liquid crystalline transitions occur at the highest temperatures; the ester also has the most thermodynamically stable crystal. It is possible that the dipolar interactions also play a role in intermolecular interactions, and that these are optimal for the carbonyl linkage.

vs. ~120° for the ester), the ether molecule has more of a kink or "dislocation" at the polar linkage. This slight alteration in geometry produces a modest decrease in in transition temperatures and concomitant increases in molecular motions. The carbonate linkage results in more drastic changes in phase behavior and molecular motions, possibly because of larger geometric, steric, and polarity changes which alter the intermolecular interactions. In fact, the NMR results show a high degree of anisotropy and relatively slow molecular motions well above the transition temperature, suggesting that the carbonate linkage blocks the cooperative interactions which induce liquid crystal formation (19) acting similarly to a separate chemical component. We further speculate that, because the physical properties of liquid and liquid crystalline ether and ester *cis* 18:1 analogues are basically similar and differ from those of the carbonate, the ester and ether may be isostructural, whereas the carbonate may have a different crystal structure.

In summary, the phase behavior and molecular motions of cholesteryl oleyl ether and cholesteryl oleate are qualitatively similar but differ in quantitative aspects. Most notably, the liquid→liquid crystalline phase transition temperature for the oleyl ester (46°C) is above, while that for the oleyl ether (31°C) is below, body temperature. However, differences between the 18:1 ester and ether in some physical properties, such as phase transition temperatures and molecular motions, are smaller than differences between the 18:1 and 18:0 ester. Cholesteryl oleyl ether is used extensively as a non-metabolizable analogue of cholesteryl oleate; however, it is generally used in small or even tracer amounts. In these cases, when the ether is diluted by cholesteryl esters, the qualitative similarities of the bulk phase physical properties of the ether and ester make the ether an apparently suitable analogue. The ether–ester intermolecular interactions should be similar to ester–ester intermolecular interactions; further, the ether should have a minimal disruption of intermolecular interactions between the cholesteryl esters, and a consequently minor effect on their physical properties. The present study does not address the properties of cholesteryl ethers in surface phases. Key events such as transport and hydrolysis of cholesteryl esters probably do not occur in the bulk phase but in or via the phospholipid-rich surface phase, where small amounts of the ester are solubilized in a preferred orientation (27, 28). Thus, an important question which remains is whether cholesteryl ethers have interfacial properties similar to esters (7).

We thank Dr. Shastri P. Bhamidipati and Dr. David Atkinson for their careful reading of the manuscript and Anne Gibbons for preparation of the manuscript. This work was supported by United States Public Health Service Grants HL26335 and HL07291.

Manuscript received 13 March 1987 and in revised form 26 May 1987.

REFERENCES

1. Deckelbaum, R. J., G. Halperin, and D. Atkinson. 1983. Thermal transitions and structural properties of synthetic cholesterol alkyl and alkenyl ethers: analogues of biological cholesterol esters. *J. Lipid Res.* **24:** 657–661.
2. Smith, E. B., and R. S. Slater. 1973. Lipids and low-density lipoproteins in intima in relation to its morphological characteristics. *Ciba Found. Symp.* **12:** 42–62.
3. Katz, S. S., G. G. Shipley, and D. M. Small. 1976. Physical chemistry of the lipids of human atherosclerotic lesions: demonstration of a lesion intermediate between fatty streaks and abdominal plaques. *J. Clin. Invest.* **58:** 200–211.
4. Deckelbaum, R. J., G. G. Shipley, and D. M. Small. 1977. Structure and interactions of lipids in human plasma low density lipoproteins. *J. Biol. Chem.* **252:** 744–754.
5. Waugh, D. A., and D. M. Small. 1984. Identification and detection of in situ cellular and regional differences of lipid composition and class in lipid-rich tissue using hot stage polarizing light microscopy. *Lab. Invest.* **51:** 702–714.
6. Funasaki, H., and J. R. Gilbertson. 1968. Isolation and identification of cholesteryl alkyl ethers from bovine cardiac muscle. *J. Lipid Res.* **9:** 766–768.
7. Stein, Y., Y. Kleinman, G. Halperin, and O. Stein. 1983. Hepatic retention and elimination of cholesteryl linoleyl ether after injection of labeled acetylated LDL or chylomicrons. *Biochim. Biophys. Acta.* **750:** 300–305.
8. Goodman, D. S., O. Stein, G. Halperin, and Y. Stein. 1983. The divergent metabolic fate of ether analogs of cholesteryl and retinyl esters after injection in lymph chylomicrons into rats. *Biochim. Biophys. Acta.* **750:** 223–230.
9. Stein, Y., O. Stein, T. Olivecrona, and G. Halperin. 1985. Putative role of cholesteryl ester transfer protein in removal of cholesteryl ester from vascular interstitium, studied in a model system in cell culture. *Biochim. Biophys. Acta.* **834:** 336–345.
10. Hamilton, J. A., N. Oppenheimer, and E. H. Cordes. 1977. Carbon-13 nuclear magnetic resonance studies of cholesteryl esters and cholesteryl ester/triglyceride mixtures. *J. Biol. Chem.* **252:** 8071–8080.
11. Quinn, D. M. 1982. Anisotropic motion of the steroid ring system of cholesteryl esters. Calculation of carbon-13 nuclear magnetic resonance relaxation times and nuclear Overhauser enhancements and comparison with experiment. *Biochemistry.* **21:** 3548–3555.
12. Ginsburg, G. S., D. M. Small, and J. A. Hamilton. 1982. Temperature-dependent molecular motions of cholesterol esters: a carbon-13 nuclear magnetic resonance study. *Biochemistry.* **21:** 6857–6867.
13. Croll, D. H., D. M. Small, and J. A. Hamilton. 1986. Temperature-dependent molecular motions of saturated acyl cholesteryl esters: a ^{13}C NMR study. *J. Chem. Phys.* **85:** 7380–7387.
14. Sripada, P. K. 1986. A simple method for the synthesis of cholesteryl ethers. *J. Lipid Res.* **27:** 352–353.
15. Pool, G. L., M. E. French, R. A. Edwards, L. Huang, and R. H. Lumb. 1982. Use of radiolabeled hexadecyl cholesteryl ether as a liposome marker. *Lipids.* **17:** 448–452.
16. Glass, C., R. C. Pittman, D. B. Weinstein, and D. Steinberg. 1983. Dissociation of tissue uptake of cholesterol ester from that of apoprotein A-I of rat plasma high density lipoprotein. *Proc. Natl. Acad. Sci. USA.* **80:** 5435–5439.
17. Halperin, G., and S. Gatt. 1980. The synthesis of cholesteryl alkyl ethers. *Steroids.* **35:** 39–42.
18. Gray, G. W. 1962. Smectic, nematic, and cholesteric

mesophases. *In* Molecular Structure and Properties of Liquid Crystals. Academic Press, New York. 42–54.
19. Croll, D. H., D. M. Small, and J. A. Hamilton. 1985. Molecular motions and thermotropic phase behavior of cholesteryl esters with triolein. *Biochemistry.* **24:** 7971–7980.
20. Small, D. M. 1970. The physical state of lipids of biological importance: cholesterol esters, cholesterol and triglyceride. *In* Surface Chemistry of Biological Systems. M. Blank, editor. Plenum Publishing Co., New York. 55–84.
21. Canet, D., G. C. Levy, and I. R. Peat. 1975. Time saving in ^{13}C spin-lattice relaxation measurement by inversion recovery. *J. Magn. Reson.* **18:** 199–204.
22. Sass, M., and D. Ziessow. 1977. Error analysis for optimized inversion recovery spin-lattice relaxation measurements. *J. Magn. Reson.* **25:** 263–276.
23. Ginsburg, G., D. Atkinson, and D. M. Small. 1984. Physical properties of cholesteryl esters. *Prog. Lipid. Res.* **23:** 135–167.
24. Woessner, D. E. 1962. Nuclear spin relaxation in ellipsoids undergoing rotational Brownian motion. *J. Chem. Phys.* **37:** 647–654.
25. Yamada, T., and E. Fukada. 1973. Non-Newtonian viscosity of liquid crystals formed by cholesteryl oleyl carbonate. *Jap. J. Appl. Phys.* **12:** 68–72.
26. Cho, S-I., and B. M. Craven. 1987. Commensurate molecules in isostructural crystals of cholesteryl *cis*- and *trans*-9-hexadecenoate. *J. Lipid Res.* **28:** 80–86.
27. Hamilton, J. A., and D. M. Small. 1982. Solubilization and localization of cholesteryl oleate in egg phosphatidylcholine vesicles. *J. Biol. Chem.* **257:** 7318–7321.
28. Spooner, P. J. R., J. A. Hamilton, D. L. Gantz, and D. M. Small. 1986. The effect of free cholesterol on the solubilization of cholesteryl oleate in phosphatidylcholine bilayers: a ^{13}C NMR study. *Biochim. Biophys. Acta.* **860:** 345–353.